Journal of Materials Chemistry

Dynamic Article Links

Cite this: *J. Mater. Chem.*, 2011, **21**, 10321

www.rsc.org/materials

PAPER

Fluorescent water-soluble responsive polymers site-specifically labeled with FRET dyes possessing pH- and thermo-modulated multicolor fluorescence emissions as dual ratiometric probes†

Xuejuan Wan and Shiyong Liu*

Received 21st January 2011, Accepted 15th March 2011
DOI: 10.1039/c1jm10332f

We reported on the synthesis of well-defined thermoresponsive polymers labeled with fluorescence resonance energy transfer (FRET) pairs at chain middle and terminals, which can act as single chain-based dual ratiometric fluorescent probes for pH and temperature under extremely dilute conditions. Starting from difunctional initiator containing a 7-nitro-2,1,3-benzoxadiazole (NBD) moiety, the atom transfer radical polymerization (ATRP) of oligo(ethylene glycol) monomethyl ether methacrylate (OEGMA) and di(ethylene glycol) monomethyl ether methacrylate (DEGMA), and the subsequent terminal group functionalization with Rhodamine B (RhB)-ethylenediamine derivative afforded thermoresponsive *NBD*-P(OEGMA-*co*-DEGMA)-RhB_2, which were labeled with FRET donor (NBD) and acceptor moieties (RhB) at the chain middle and terminals. The fluorescence emission of terminal RhB functionalities is highly pH-dependent, *i.e*, non-fluorescent in neutral or alkaline media (spirolactam form) and highly fluorescent in acidic media (ring-opened acyclic form), thus the off/on switching of FRET process can be facilely modulated by solution pH. Moreover, at acidic pH and highly dilute conditions, the thermo-induced chain collapse and extension of *NBD*-P(OEGMA-*co*-DEGMA)-RhB_2 can effectively modulate the spatial distance between FRET donor and acceptor moieties, leading to prominent changes in FRET efficiencies. The site-specific incorporation of one FRET donor and two pH-switchable acceptors at the chain middle and terminals of thermoresponsive polymers allows for the effective off/on switching and the modulation of efficiency of FRET processes by dually playing with solution pH and temperatures. This work represents the first report of single thermoresponsive polymer chains acting as dual ratiometric fluorescent probes under highly dilute conditions.

1. Introduction

In living organisms, pH and temperature exhibit crucial effects on the cell and tissue activities, and abnormal pH and temperature deviations in bio-microenvironments are typically associated with pathological processes and dysfunctions.[1–3] For example, normal tissues possess a pH range of ~7.2–7.4, whereas certain tumor tissues have lower extracellular pH (~6.0–6.5);[4] moreover, pathological cells might have higher temperature than normal cells due to enhanced metabolic activities in the former.[5,6] Thus, the accurate monitoring of temperature and pH variations and gradients are quite crucial for the diagnosis of certain diseases, the determination of pathogenesis, and the measurement of pharmaceutical therapy efficiencies.

During the past decade, a variety of fluorometric pH and temperature detection systems have been reported,[7–13] and most of them were based on the monitoring of changes in the relative fluorescence emission intensity of a single emission peak. Currently, the fluorescence resonance energy transfer (FRET) principle, which refers to the non-radiative energy transfer between fluorescent donors and acceptors, has been typically employed for the construction of ratiometric fluorescent pH and thermal probes to effectively eliminate the interference from background signals and the fluctuation of detection conditions.[14–21] Recently, Krishnan *et al.*[22] reported a pH-triggered DNA nanomachine labeled with FRET donor and acceptor at the two terminals. The designed DNA duplex adopts an extended conformation at pH 7.3 and a "closed state" at pH 5. Thus, the mapping of spatial and temporal pH variations within living cells can be successfully achieved.

Stimuli-responsive polymers,[23] which are capable of exhibiting reversible or irreversible changes in physical properties and/or chemical structures to variations in external environment, have recently been introduced into the design of novel fluorometric

CAS Key Laboratory of Soft Matter Chemistry, Department of Polymer Science and Engineering, Hefei National Laboratory for Physical Sciences at the Microscale, University of Science and Technology of China, Hefei, Anhui, 230026, China. E-mail: sliu@ustc.edu.cn

† Electronic supplementary information (ESI) available: Supplementary fig. S1. See DOI: 10.1039/c1jm10332f

sensing systems.[24–31] This combination can achieve multifunctional integration, improved water-solubility, and biocompatibility, as compared to small molecule derivatives of fluorescent dyes. In this context, Frey and Duan reported the synthesis of hybrid gold nanoparticles coated with *N*-isopropylacrylamide (NIPAM)-functionalized hyperbranched polyglycerol.[32] Since the phase transition behavior of hybrid nanoparticle dispersion is highly dependent on solution conditions, they can serve as a prototype of dual pH and thermal sensors. Uchiyama *et al.*[26] reported the construction of fluorescent temperature and pH sensors based on a multi-responsive copolymer containing a polarity-sensitive dye (DBDAE). The pH- and thermo-induced aggregation of responsive polymer chains leads to the formation of hydrophobic domains in which the fluorescence emission of DBDAE dyes can be dramatically enhanced. We recently reported the incorporation of Hg^{2+} and pH-reactive dyes into the thermoresponsive block of a double hydrophilic block copolymer (DHBC), and found that the polymeric micelle-based sensing system exhibits enhanced detection efficiencies towards pH, temperature, and Hg^{2+} ions.[33] However, the above two examples are both based on changes in relative fluorescence emission intensities of a single emission band. Moreover, these thermo- or pH-induced aggregates and polymeric assemblies are only stable under specific pH and temperature ranges, and the deviation of solution condition from this range will lead to the decrease of detection performance. To solve these issues, structurally stable hybrid nanoparticles functionalized with responsive polymer brushes and stimuli-triggered conformational changes (collapse and swelling) of single responsive polymer chains have been utilized to fabricate novel detection systems.[34,35]

Concerning hybrid nanoparticles-based probes, we recently reported the construction of colorimetric and fluorometric thermal sensors on the basis of hybrid silica nanoparticles grafted with thermoresponsive PNIPAM brushes with the inner and outer layers labeled with 7-nitro-2,1,3-benzoxadiazole (NBD) and spiropyran (SP) moieties, which display irradiation-regulated off–on switchable FRET processes.[34] Under UV irradiation and upon heating, the collapse of the PNIPAM brush leads to decreased spatial distances between NBD (FRET donor) in the inner layer and the ring-opened merocyanine form of SP (FRET acceptor) in the outer layer. As the FRET efficiency is strongly dependent on the relative distance between FRET pairs,[36,37] this process can be employed to fabricate colorimetric and ratiometric fluorescent thermal sensors with switchable FRET processes. Just recently, Chujo *et al.*[35] reported a fluorescent temperature sensor based on hybrid Au nanoparticles coated with thermoresponsive PNIPAM brush. The periphery of PNIPAM brush was labeled with boron dipyrromethene (BODIPY). Thermo-induced collapse and swelling of PNIPAM brushes can effectively modulate the spatial distance between fluorescent dyes and Au nanoparticles; therefore, the extent of fluorescence quenching of BODIPY emission by Au nanoparticles can be utilized to design fluorescent thermal sensors.

Under highly dilute conditions, the pH- or thermo-induced conformational changes (chain collapse/extension) of single responsive polymer chains, upon appropriate dye labeling at predetermined positions,[38–40] can also be exploited to design sensing systems. Jo *et al.*[41] synthesized pH-sensitive poly(methacryloyl sulfadimethoxine) (PSDM) labeled with pyrene and coumarin 343 dyes at chain terminals. As the FRET efficiency between pyrene and coumarin 343 is highly dependent on the chain conformation and solution pH, the reported system can serve as sensitive pH probes. In another example, they further labeled thermoresponsive PNIPAM with pyrene and fluorescent quencher C_{60} and reported that the quenching efficiency can be considerably enhanced at elevated temperatures if more quencher moieties are covalently incorporated into polymer chains.[42] Just recently, Zentel *et al.*[43] reported another example of ratiometric fluorescent thermal sensor based on thermoresponsive poly(di(ethylene glycol) monomethyl ether methacrylate) (PDEGMA) labeled with FRET donor and acceptor dyes. The thermo-induced single chain collapse of dye-labeled PDEGMA can be facilely monitored by changes in fluorescence intensity ratios.

It is worthy of noting that most of the responsive polymer chain-based fluorescent ratiometric sensors are only applicable to single sensing functions such as pH or temperatures. Fluorescent responsive polymers with dual (pH and temperature) or multiple sensing capabilities are highly desirable considering their potential applications under complex conditions (*e.g.*, intracellular). Besides, if one FRET donor and two or multiple stimuli-switchable acceptor dyes are labeled into responsive polymers at predetermined positions, more effective and versatile modulation of FRET processes can be expected. Finally, thermoresponsive polymers employed in the above examples only involve PNIPAM and PDEGMA homopolymers, which possess fixed phase transition temperatures; thus it is quite advantageous to design sensing systems with tunable thermal detection ranges.

Aiming at solving the above issues and developing a biocompatible and highly sensitive ratiometric fluorescent probe for pH and temperatures, herein we report on the synthesis of thermoresponsive polymers labeled with one FRET donor (NBD) and two off/on pH-switchable fluorescent acceptor dyes, Rhodamine B-ethylenediamine derivative,[33,44–46] at chain middle and terminals (Scheme 1). Variations in solution pH and temperatures can be facilely monitored by changes in fluorescence intensity ratios due to thermo-regulated spatial distance between the FRET pair and pH-modulated off–on switchable

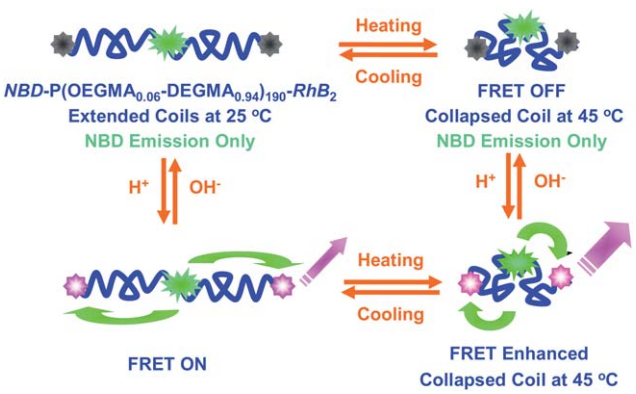

Scheme 1 Schematic illustration of pH- and thermo-modulation of FRET processes in the aqueous solution of well-defined thermoresponsive polymer, *NBD*-P(OEGMA-*co*-DEGMA)-*RhB*$_2$, which were labeled with NBD and pH-reactive RhB moieties at the chain middle and terminals, respectively.

FRET processes, resulting from the thermo-induced collapse/swelling of dye-labeled single responsive polymer chains under highly dilute conditions and the pH-induced transformation of Rhodamine B-ethylenediamine derivative between non-fluorescent spirolactam (in neutral and alkaline media) and highly fluorescent acyclic forms (under acidic conditions). It should be noted that the reported ratiometric fluorescent probes possess dual detection capabilities for pH and temperature under extremely dilute conditions, which augurs well for their potential applications in sensing, bioimaging, and clinical diagnosis.

2. Experimental section

Materials

Oligo(ethylene glycol) monomethyl ether methacrylate (OEGMA, M_n = 475, mean degree of polymerization, DP, is 8–9) and di(ethylene glycol) methyl ether methacrylate (DEGMA) were purchased from Aldrich and purified by passing through a short silica column (100–200 mesh) and stored at −20 °C prior to use. 4-Chloro-7-nitrobenzofurazan (NBD-*Cl*, Alfa, 99%), Rhodamine B (RhB, Acros), 2-bis(hydroxymethyl) propionic acid (*bis*-MPA, Aldrich, 98%), 2-bromoisobutyryl bromide (Aldrich, 97%), 2,2′-dimethoxy-opane (Aldrich, 98%), copper(I) bromide (CuBr, Aldrich, 99.999%), and 2,2′-bipyridine (bpy, Alfa, 99%) were used as received. Dowex 50W × 8–200 ion exchange resin was purchased from Lancaster and used as received. *N*,*N*′-Dicyclohexylcarbodiimide (DCC), 4-(dimethylamino) pyridine (DMAP), and all other reagents were purchased from Sinopharm Chemical Reagent Co. and used as received. Bis(hydroxymethyl) propionic acid acetonide (*bis*-MPA acetonide),[47] Rhodamine B-ethylenediamine derivative (RhB-NH_2),[48] and 4-(2-hydroxyethyl-amino)-7-nitrobenzofurazan (NBD-*OH*)[49] were synthesized according to literature procedures (Scheme 2).

Sample preparation

General approaches employed for the synthesis of difunctional initiator, NBD-(*Br*)$_2$, and FRET pair-labeled thermoresponsive polymer, *NBD*-P(OEGMA-*co*-DEGMA)-*RhB*$_2$, are shown in Scheme 2.

Synthesis of NBD-based difunctional initiator NBD-(Br)$_2$. *Bis*-MPA acetonide (0.87 g, 5.0 mmol), DCC (1.13 g, 5.5 mmol), DMAP (73 mg, 0.6 mmol), and 80 mL anhydrous CH_2Cl_2 were added to a 250 mL dry round-bottomed flask and then the flask was immersed into an ice water bath. A solution of NBD-*OH* (1.12 g, 5.0 mmol) in 50 mL anhydrous CH_2Cl_2 was slowly added *via* a dropping funnel over 30 min under magnetic stirring. The reaction mixture was stirred for 1 h in an ice water bath and then overnight at room temperature. After filtration, all the solvents were removed by rotary evaporation. The crude product was subjected to column chromatography purification (silica gel, CH_2Cl_2 as eluent). NBD-(*bis*-MPA acetonide) was obtained after drying overnight in a vacuum oven (1.60 g, 84.2% yield). ^{1}H NMR ($CDCl_3$, δ, ppm; Fig. 1a): 8.51, 6.46 (2H, benzofurazan-*H*), 6.63 (1H, –N*H*CH_2–), 4.74 (2H, –NHCH_2CH_2O–), 4.22, 3.67 (4H, –CH_2OC(CH_3)$_2$OCH_2–), 3.94 (2H, –NHCH_2CH_2O–), 1.42 (6H, –C(CH_3)$_2$), 1.23 (3H, O═CCCH_3).

Dowex 50W × 8–200 ion exchange resin (3.0 g) was added into a solution of NBD-(*bis*-MPA acetonide) (1.33 g, 3.5 mmol) in 100 mL methanol and the mixture was stirred at 40 °C for 4 h. The ion exchange resin was then filtered off and washed with methanol three times. The filtrate was concentrated and dried under vacuum to afford NBD-(*bis*-MPA) (1.12 g, 94.1% yield). ^{1}H NMR ($CDCl_3$, δ, ppm; Fig. 1b): 8.49, 6.46 (2H, benzofurazan-*H*), 6.64 (1H, –N*H*CH_2–), 4.74 (2H, –NHCH_2CH_2O–), 4.19, 3.67 (4H, –OOCC(CH_2OH)CH_2OH), 3.94 (2H, –NHCH_2CH_2O–), 1.09 (3H, O═CCCH_3).

NBD-(*bis*-MPA) (0.68 g, 2.0 mmol), TEA (0.42 g, 4.2 mmol), and 40 mL anhydrous THF were added to a 100 mL dry round-bottomed flask. After the flask was cooled to 0 °C in an ice water bath, 2-bromoisobutyryl bromide (0.97 g, 4.2 mmol) in 10 mL THF was slowly added *via* a dropping funnel over 30 min. The reaction mixture was stirred in an ice water bath for another 1 h and then overnight at room temperature. After filtration, most of the solvent was removed on a rotary evaporator. The crude product was then dissolved in CH_2Cl_2 and washed with saturated aqueous solution of $NaHCO_3$ three times. The organic layer was collected and dried over anhydrous $MgSO_4$. The filtrate was concentrated and then subjected to column chromatography (silica gel, CH_2Cl_2 as eluent). The eluent was collected and evaporated to dryness under vacuum to obtain NBD-based difunctional initiator NBD-(*Br*)$_2$ (0.97 g, 76.0% yield). ^{1}H NMR ($CDCl_3$, δ, ppm; Fig. 1c): 8.45, 6.22 (2H, benzofurazan-*H*), 6.64 (1H, –N*H*CH_2–), 4.47 (2H, –NHCH_2CH_2O–), 4.28 (4H, O═CCCH_2OC═O), 3.81 (2H, –NHCH_2CH_2O–), 2.92 (2H, –CH_2O*H*), 1.83 (12H, O═CC(CH_3)$_2$Br), 1.34 (3H, O═CCCH_3).

Synthesis of NBD-P(OEGMA-*co*-DEGMA)-Br$_2$. DEGMA (2.63 g, 14.0 mmol), OEGMA (0.48 g, 1.0 mmol), bpy (31 mg, 0.2 mmol), and NBD-(*Br*)$_2$ (32 mg, 0.05 mmol) were introduced into a glass ampoule containing 2 mL 2-propanol. After degassing through three freeze–thaw cycles, CuBr (14 mg, 0.1 mmol) was added and the glass ampoule was sealed under vacuum. The polymerization was carried out at room temperature for 4 h, and then terminated by immersing into liquid nitrogen. The reaction mixture was then diluted with THF and passed through a neutral alumina column to remove the catalyst. The eluent was concentrated and precipitated into diethyl ether. The sediments were then collected and dried in a vacuum oven to constant weight at room temperature (1.92 g, 60.5% yield). The molecular weight and molecular weight distribution of *NBD*-P(OEGMA-*co*-DEGMA)-*Br*$_2$ were determined by DMF GPC: M_n = 19 500, M_w/M_n = 1.11 (Fig. 2). The overall DP of *NBD*-P(OEGMA-*co*-DEGMA)-*Br*$_2$ was determined to be 190 and the molar fractions of OEGMA and DEGMA residues were determined to be 0.06 and 0.94, respectively, by ^{1}H NMR analysis in $CDCl_3$. The obtained copolymer was thus denoted as *NBD*-P(OEGMA$_{0.06}$-*co*-DEGMA$_{0.94}$)$_{190}$-*Br*$_2$.

Synthesis of NBD-P(OEGMA-*co*-DEGMA)-RhB$_2$. *NBD*-P(OEGMA-*co*-DEGMA)-*Br*$_2$ (1.5 g, 0.076 mmol Br), RhB-NH_2 (0.073 g, 0.15 mmol), TEA (20 mg, 0.2 mmol) and 30 mL DMF were added into a 100 mL round-bottomed flask. The reaction mixture was allowed to stir at 45 °C for 48 h. After removing all the solvents at reduced pressure, the residues were dissolved in THF and then precipitated into an excess of anhydrous diethyl

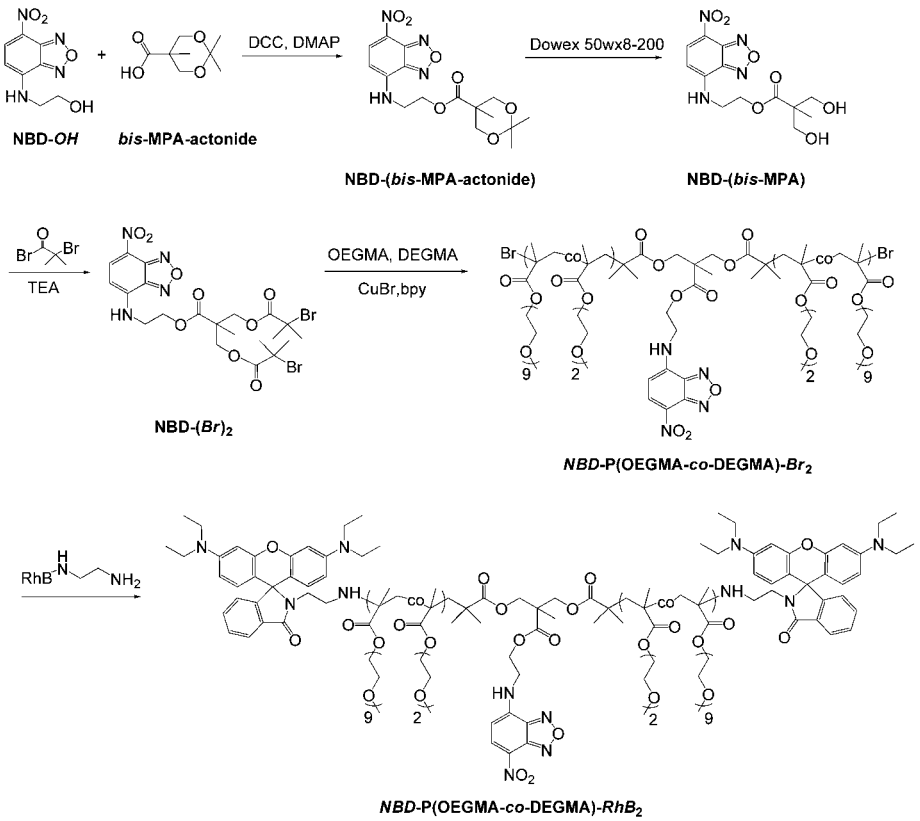

Scheme 2 Synthetic routes employed for the synthesis of NBD-$(Br)_2$ and *NBD*-P(OEGMA-*co*-DEGMA)-RhB_2 *via* atom transfer radical polymerization (ATRP).

ether. The obtained product was dried overnight in a vacuum oven to constant weight (1.36 g, 90.6% yield). The molecular weight and molecular weight distribution of *NBD*-P$(OEGMA_{0.06}$-*co*- $DEGMA_{0.94})_{190}$-RhB_2 were determined by GPC using DMF as eluent: $M_n = 21\,000$, $M_w/M_n = 1.13$ (Fig. 2).

Characterization

^{1}H NMR spectra were recorded on a Bruker 300 MHz spectrometer using $CDCl_3$ as solvent. Molecular weights and molecular weight distributions were determined by gel permeation chromatography (GPC) equipped with a Waters 1515 pump and a Waters 2414 differential refractive index detector (set at 30 °C). It used a series of three linear Styragel columns (HT2, HT4, and HT5) at an oven temperature of 45 °C. The eluent was DMF at a flow rate of 1.0 mL min^{-1}. All UV-Vis spectra were acquired on a Unico UV-Vis 2802PCS spectrophotometer. The transmittance of the aqueous solution was acquired at a wavelength of 600 nm. The cloud point was defined as the temperature corresponding to 1% decrease of optical transmittance. Laser light scattering (LLS) measurements were conducted on a commercial spectrometer (ALV/DLS/SLS-5022F) equipped with a multi-tau digital time correlator (ALV5000) and a cylindrical 22 mW UNIPHASE He–Ne laser (λ_0 = 632 nm) as the light source. Fluorescent images were recorded under inverted fluorescence microscopy (Olympus I × 71) equipped with a temperature-regulated incubator (450–480 nm exciter filter and long pass 515 nm barrier filter). Fluorescence spectra were recorded using a RF-5301/PC (Shimadzu) spectrofluorometer. The temperature of the water-jacketed cell holder was controlled by a programmable circulation bath. The slit widths were set at 5 nm for excitation and 5 nm for emission. To estimate the FRET efficiency (E) between NBD and RhB moieties, we employed a simplified equation, $E = 1 - I/I_0$, where I_0 is the NBD donor fluorescence intensity (525 nm) at pH 10 and 25 °C, and I is the NBD fluorescence intensity after external stimuli (*e.g.* pH and temperature) were actuated.[46]

3. Results and discussion

General approaches employed for the synthesis of difunctional initiator NBD-$(Br)_2$ and well-defined thermoresponsive polymer respectively labeled with FRET pairs at chain middle and terminals, *NBD*-P(OEGMA-*co*-DEGMA)-RhB_2, are shown in Scheme 2. Under neutral pH condition, *NBD*-P(OEGMA-*co*-DEGMA)-RhB_2 in aqueous solution only exhibits the fluorescence emission of NBD as the RhB moieties exist in the non-fluorescent spirolactam form. As the solution pH decreased, pH-reactive RhB moieties at chain terminals are subjected to selective ring-opening reaction, producing highly fluorescent acyclic species.[33,46] Therefore, the FRET process between NBD/RhB FRET pair is off/on switchable *via* pH variations. Most importantly, the incorporation of one FRET donor and two pH-switchable acceptors at the chain middle and terminals of the thermoresponsive polymer allows for the effective modulation of FRET efficiencies by utilizing the thermo-induced single chain collapse of *NBD*-P(OEGMA-*co*-DEGMA)-RhB_2 under highly dilute conditions. Thus, the current design of site-specifically

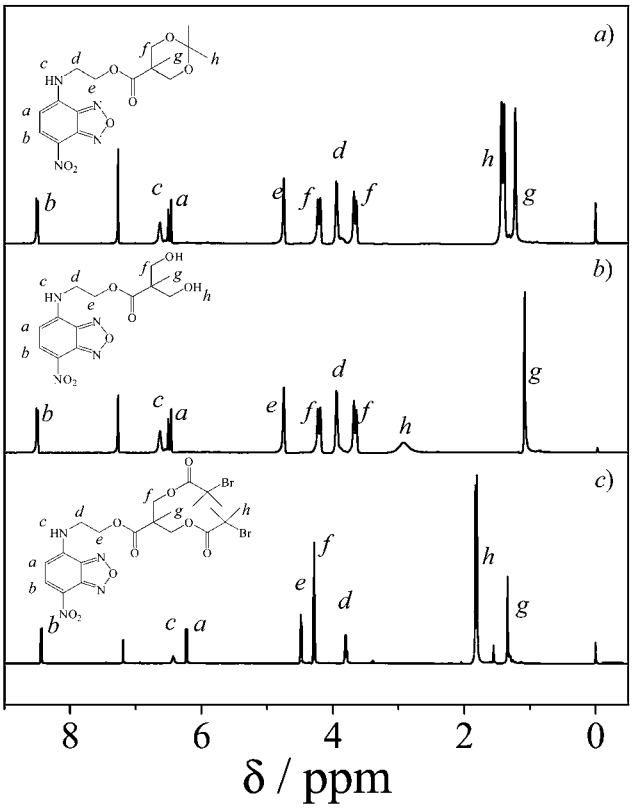

Fig. 1 ^{1}H NMR spectra recorded in $CDCl_3$ for (a) NBD-(*bis*-MPA acetonide), (b) NBD- (*bis*-MPA), and (c) NBD-$(Br)_2$.

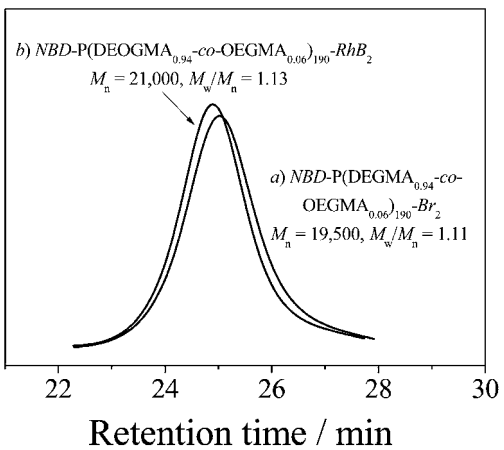

Fig. 2 DMF GPC traces recorded for (a) *NBD*-P(OEGMA$_{0.06}$-*co*-DEGMA$_{0.94}$)$_{190}$-Br_2, and (b) *NBD*-P(OEGMA$_{0.06}$-*co*-DEGMA $_{0.94}$)$_{190}$-RhB_2.

dye-labeled thermoresponsive polymers allows for the construction of dual ratiometric fluorescent probes for pH and temperatures (Scheme 1).

Synthesis of NBD-$(Br)_2$ and thermoresponsive NBD-P (OEGMA-*co*-DEGMA)-RhB_2

NBD-based difunctional atom transfer radical polymerization (ATRP) initiator, NBD-$(Br)_2$, was synthesized in three steps as illustrated in Scheme 2. NBD-*OH* was first reacted with *bis*-MPA acetonide *via* DCC-mediated esterification. After the acetonide protecting group of NBD-(*bis*-MPA acetonide) was removed after treating with Dowex 50W × 8–200 ion exchange resin, the obtained NBD-(*bis*-MPA) was further reacted with 2-bromoisobutyryl bromide to afford NBD-$(Br)_2$. ^{1}H NMR spectra of NBD-(*bis*-MPA acetonide), NBD-(*bis*-MPA), and NBD-$(Br)_2$ are shown in Fig. 1, together with the peak assignments. After the esterification reaction, resonance signals of methylene protons in NBD-*OH* shifted from 3.28 ppm to 4.75 ppm (peak *e*, Fig.1a). After the deprotection step, resonance signals of methyl protons ascribed to the acetonide functionality completely disappeared (peak *h*, Fig. 1b). After the esterification reaction of NBD-(*bis*-MPA) with 2-bromoisobutyryl bromide, resonance signals of methylene protons neighboring to hydroxyl groups (peak *f*, 3.68 and 4.19 ppm; Fig. 1b) completely disappeared, accompanied with the appearance of new resonance signal at 4.29 ppm in the NMR spectrum of NBD-$(Br)_2$ (peak *f*, Fig. 1c). Moreover, we can also observe the appearance of new resonance signal at 1.83 ppm (peak *h*; Fig. 1c), which are ascribed to methyl protons in the 2-bromoisobutyryl moiety. Peak assignments and peak integral ratios between characteristic resonance signals all confirmed the successful synthesis of NBD-based difunctional initiator, NBD-$(Br)_2$ (Fig. 1).

NBD-labeled thermoresponsive polymer, *NBD*-P(OEGMA-*co*-DEGMA)-Br_2, was prepared *via* ATRP by utilizing NBD-$(Br)_2$ as the initiator. The bromide terminal groups were modified with RhB-NH_2 to afford the target FRET pair-labeled thermoresponsive polymer, *NBD*-P(OEGMA-*co*-DEGMA)-RhB_2. The ^{1}H NMR spectrum of *NBD*-P(OEGMA-*co*- DEGMA)-Br_2 is shown in Fig. 3a, together with the peak assignments. On the basis of the integral ratio of peaks *a* to *b*, the molar fractions of OEGMA and DEGMA residues were determined to be 0.06 and 0.94, respectively. Similarly, the overall DP of the polymer was

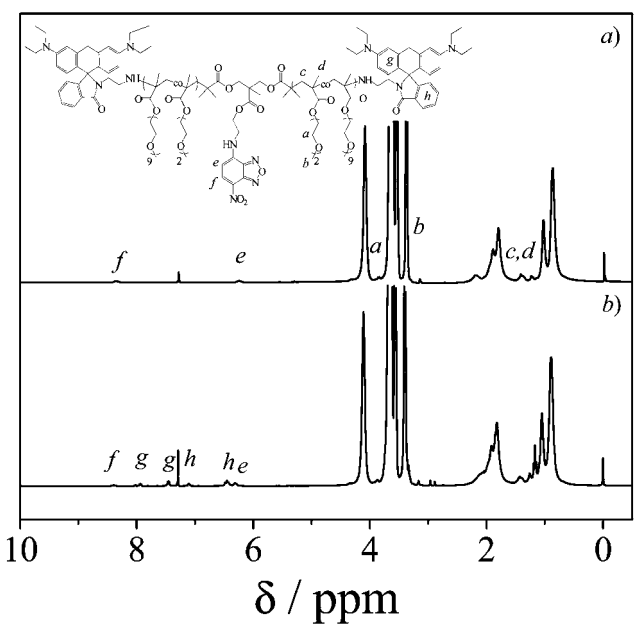

Fig. 3 ^{1}H NMR spectra recorded for (a) *NBD*-P(OEGMA$_{0.06}$-*co*-DEGMA$_{0.94}$)$_{190}$-Br_2, and (b) *NBD*-P(OEGMA$_{0.06}$-*co*-DEGMA$_{0.94}$)$_{190}$-RhB_2 in $CDCl_3$.

determined to 190 by ^{1}H NMR analysis. Thus, the obtained random copolymer was denoted as *NBD*-P(OEGMA$_{0.06}$-*co*-DEGMA$_{0.94}$)$_{190}$-*Br*$_2$. DMF GPC trace of *NBD*-P(OEGMA$_{0.06}$-*co*- DEGMA$_{0.94}$)$_{190}$-*Br*$_2$ precursor is shown in Fig. 2, revealing a relatively sharp and symmetric peak with no tailing or shoulder at the lower or higher molecule weight side, indicating that the ATRP process was conducted in a controlled manner.

The subsequent terminal group functionalization of *NBD*-P(OEGMA-*co*-DEGMA)-*Br*$_2$ with Rhodamine B (RhB)-ethylenediamine derivative, RhB-NH$_2$, was conducted in DMF at 45 °C for 4 h.[41] ^{1}H NMR spectrum of *NBD*-P(OEGMA-*co*-DEGMA)-*RhB*$_2$ is shown in Fig. 3b, and all the resonance signals ascribing to RhB moiety can be clearly discerned and well assigned. On the basis of the integral ratio between peaks *f* and *g*, which are characteristic of NBD and RhB moieties, the degree of terminal Br group transformation was determined to be ~93%. Compared to that of *NBD*-P(OEGMA-*co*-DEGMA)-*Br*$_2$, DMF GPC trace of *NBD*-P(OEGMA-*co*-DEGMA)-*RhB*$_2$ exhibited a slight shift towards the higher molecular weight side (Fig. 2). In addition, the GPC trace was again mono-modal and quite symmetric, suggesting that the terminal group transformation reaction does not affect structural integrity of the precursor polymer.

Thermal phase transition behavior of NBD-P(OEGMA-*co*-DEGMA)-RhB$_2$

Possessing two ethylene oxide repeating units in the monomer, PDEGMA homopolymer possesses a lower critical solution temperature (LCST) phase transition at ~26 °C,[50–52] just like those exhibited by PNIPAM in aqueous solutions (LCST ~ 32 °C).[53] PDEGMA molecularly dissolves in cold and dilute aqueous solution but becomes insoluble above the LCST. On the other hand, POEGMA, with ~8–9 ethylene oxide repeating units in the monomer, is highly hydrophilic. It has been well-established that the copolymerization of OGEMA with DEGMA leads to the facile tuning of LCST in the range of 26–90 °C for the copolymer.[50,51,54] In the current work, we focused on the development of single thermoresponsive polymer chain-based dual ratiometric fluorescent probes for pH and temperature. Thus, we need to determine at first the suitable concentration range at which thermo-induced single chain collapse can be observed. Temperature dependence of optical transmittance at 700 nm recorded for the *NBD*-P(OEGMA-*co*-DEGMA)-*RhB*$_2$ aqueous solution at varying concentrations are shown in Fig. 4. We can clearly observe that the cloud points increase with decreasing polymer concentrations, accompanied with the broadening of transition temperature range. At a concentration of 2.0 g L^{-1}, the aqueous solution of *NBD*-P(OEGMA-*co*-DEGMA)-*RhB*$_2$ exhibits a relatively sharp decrease of optical transmittance above ~35 °C, and the cloud point shifts to ~38 °C at a polymer concentration of 0.05 g L^{-1}. At a concentration down to 1.0 mg L^{-1}, we can not observe any changes in optical transmittance in the whole temperature range investigated (30–50 °C). Further examination of the aqueous solution of *NBD*-P(OEGMA-*co*-DEGMA)-*RhB*$_2$ aqueous solution by LLS revealed that the scattered light intensity at a scattering angle of 15° exhibits negligible changes in the temperature range of 30–50 °C (Inset in Fig. 4), suggesting that at such a low

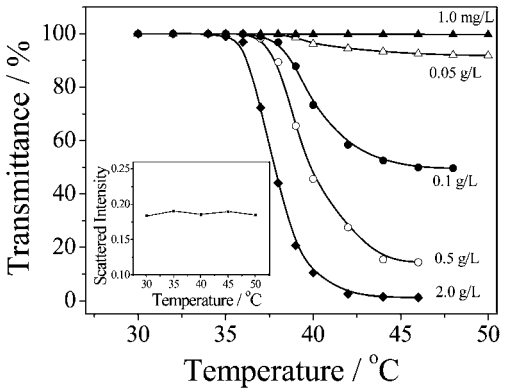

Fig. 4 Temperature dependence of optical transmittance at 700 nm obtained for *NBD*-P(OEGMA$_{0.06}$-*co*-DEGMA$_{0.94}$)$_{190}$-*RhB*$_2$ aqueous solutions at varying polymer concentrations. The cloud point was defined as the temperature corresponding to 1% decrease of optical transmittance. The inset shows the temperature dependence of scattered light intensity at a scattering angle of 15° recorded for 1.0 mg L^{-1} aqueous solution of *NBD*-P(OEGMA-*co*-DEGMA)-*RhB*$_2$.

concentration, thermoresponsive polymers exist as isolated single chains and interchain aggregation does not occur. This is reasonable considering that a large increase in scattered light intensity should have been observed if interchain aggregation occurs since the scattering intensity is proportional to the square of the mass of scattering objects. However, considering the thermoresponsive nature of *NBD*-P(OEGMA-*co*-DEGMA)-*RhB*$_2$, single chain collapse will surely occur at elevated temperatures, which were further employed in the subsequent section to construct ratiometric fluorescent thermal probes by taking advantage of the fact that chain collapse will considerably reduce the spatial distance between FRET donor and acceptors.

Dual ratiometric fluorescent sensing for pH and temperatures

When responsive polymer chains were labeled with FRET pairs, external stimuli-triggered conformational changes, *i.e.*, chain collapse/swelling or aggregation are associated with changes in spatial distance between FRET donors and acceptors, which can be further quantified by the efficiency of FRET processes. In a series of work by Jo and his coworkers,[41,42,55–58] they developed single polymer chain-based pH or temperature probes by employing pH- or thermo-responsive polymers labeled with appropriate dyes. In this work we aim at developing a dual ratiometric fluorescent probe on the basis of single thermoresponsive polymer chains of *NBD*-P(OEGMA-*co*-DEGMA)-*RhB*$_2$, which were labeled with one FRET donor (NBD) and two potential FRET acceptor dyes (RhB-ethylenediamine dyes). The fluorescence emission of RhB-ethylenediamine derivative is highly dependent on solution pH. It is non-fluorescent in neutral or alkaline media (spirolactam form) and highly fluorescent in acidic media (ring-opened acyclic form), thus the off/on switching of FRET process can be facilely modulated by solution pH.[33,46] Moreover, at acidic pH and highly dilute conditions, the thermo-induced reversible chain collapse and extension of *NBD*-P(OEGMA-*co*- DEGMA)-*RhB*$_2$ can effectively modulate the spatial distance between FRET donor and acceptor moieties, leading to prominent changes in fluorescence intensity ratios (Scheme 1).

The fluorescence emission spectra recorded for 1.0 mg L^{-1} aqueous solution (pH 9) of *NBD*-P(OEGMA-*co*-DEGMA)-RhB_2 at varying temperatures are shown in Fig. 5. Under this condition, the RhB moiety is non-fluorescent and we can only observe the emission band of NBD moiety at ~525 nm. In the temperature range of 28–45 °C, the fluorescence intensity at 525 nm exhibits ~30% decrease. This is quite perplexing as we expected the increase of emission intensity of NBD since the thermo-induced chain collapse of P(OEGMA-*co*-DEGMA) can lead to the formation of hydrophobic microenvironment. Previously, Uchiyama *et al.*[24,59–61] reported that NBDAE or DBDAE-labeled PNIPAM exhibits enhanced emission at temperatures above the thermal phase transition temperature; for NBDAE-labeled PNIPAM microgels, a similar trend of temperature-dependent fluorescence emission intensity was also observed. Preliminary experiments revealed that even for *NBD*-P(OEGMA-*co*-DEGMA) at a concentration as high as 0.5 g L^{-1} and pH 9, under which condition heating across the LCST will lead to the formation of mesoglobule aggregates, we can still observe the decrease of emission intensity with increasing temperatures. It seems that the polymer matrix, *i.e.*, P(OEGMA-*co*-DEGMA) *versus* PNIPAM, can exhibit considerable effects on the quantum yield at temperatures spanning across the LCST, though both of them are thermoresponsive and possess similar

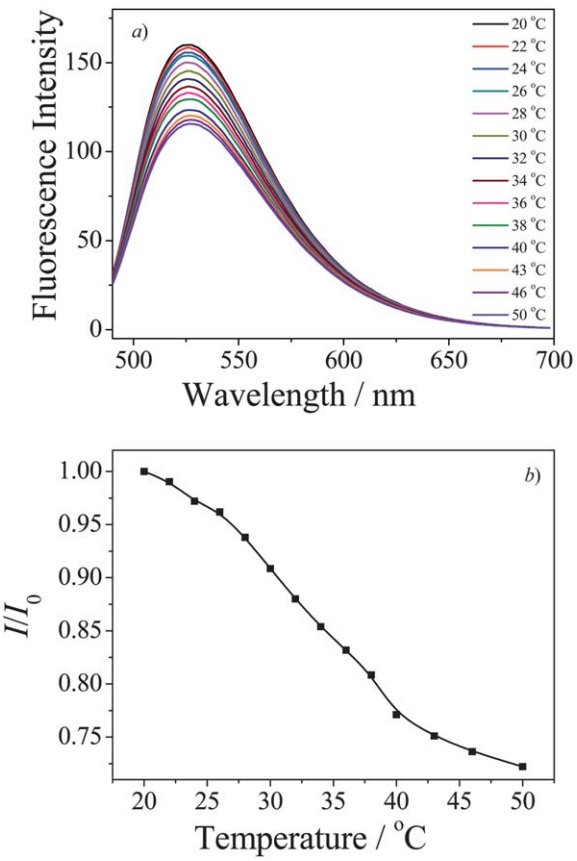

Fig. 5 (a) Fluorescence emission spectra and (b) relative fluorescence intensity changes (pH 9, $\lambda_{ex} = 470$ nm, $\lambda_{em} = 525$ nm; slit widths: Ex 5 nm, Em 5 nm) recorded for 1.0 mg L^{-1} aqueous solution of *NBD*-P$(OEGMA_{0.06}$-*co*-$DEGMA_{0.94})_{190}$-RhB_2 in the temperature range of 20–50 °C.

LCST phase transition behavior. A possible explanation is that the fluorescence emission of polarity-sensitive dyes such as NBDAE labeled onto thermoresponsive polymer chains are actually determined by two competitive factors, namely the intrinsic decrease of quantum yield at elevated temperatures[62] and the emission enhancement within thermo-induced hydrophobic domains. In the case of NBDAE-labeled PNIPAM, the latter factor dominates; whereas in the case of *NBD*-P(OEGMA-*co*-DEGMA)-RhB_2, the former factor is the dominating one.

As the solution pH decreased to below ~6, the ring-opening reaction of RhB-ethylenediamine moiety initially in the spirolactam form transforms to the highly fluorescent RhB species in the acyclic form, and the fluorescence emission band of NBD overlaps well with the absorbance band of RhB moieties (see Fig. S1†), which can effectively switch on the FRET process between NBD and RhB moieties. The temperature dependent fluorescence spectra recorded for 1.0 mg L^{-1} aqueous solution of *NBD*-P(OEGMA-*co*-DEGMA)-RhB_2 at pH 2 in the temperature range of 25–45 °C are shown in Fig. 6. We can apparently observe two well-resolved emission peaks at ~525 nm and 593 nm, which should be ascribed to the fluorescence emission of NBD and acyclic RhB moieties. Moreover, it is clearly evident that the emission band of NBD (FRET donor) decreases with increasing temperatures, accompanied with the increase of emission intensity of acyclic RhB (FRET acceptor) in the same temperature range.

In the range of 25–30 °C at pH 2, which are below the LCST of *NBD*-P(OEGMA-*co*- DEGMA)$_{190}$-RhB_2 copolymer, the polymer chains exist as extended coils, *i.e.*, the spatial distance between the FRET pair are relatively large, leading to the relatively low FRET efficiency ($E \sim 7.6\%$, $F_{593}/F_{525} \sim 0.34$ at 25 °C). At temperatures above the LCST, chain collapse of *NBD*-P(OEGMA-*co*-DEGMA)$_{190}$-RhB_2 copolymer in aqueous solution occurs, leading to the prominent decrease of spatial distance between NBD and RhB moieties and the enhanced FRET efficiency ($E \sim 62.6\%$, $F_{593}/F_{525} \sim 2.1$ at 45 °C). The fluorescence intensity ratio between RhB and NBD emission bands exhibit ~6.2-fold increase in the temperature rang of 25–45 °C (Fig. 6b). Most importantly, most of the increase in emission intensity ratios actually occurs in the relatively narrow range of 35–40 °C, which is quite close to the physiological conditions. It should be noted that the optimum temperature detection range of *NBD*-P(OEGMA-*co*-DEGMA)-RhB_2 can be facilely adjusted by varying the composition of *NBD*-P(OEGMA-*co*-DEGMA)-RhB_2 copolymer, which can tune the LCST phase transitions in the range of 26 °C to ~90 °C depending on the molar contents of OEGMA residues.[50–52] In addition, from the inset of Fig. 6, we can clearly discern the fluorometric transition from green to orange under an inverted fluorescence microscopy upon heating from 25 °C to 45 °C at pH 2. Based on the above results, we have established that *NBD*-P(OEGMA-*co*-DEGMA)-RhB_2 in aqueous solution can serve as single chain-based sensitive ratiometric fluorescent thermometers under low pH and highly dilute conditions.

Fig. 7 shows the pH dependence of fluorescence spectra and emission intensity ratios, F_{593}/F_{525}, recorded for 1.0 mg L^{-1} aqueous solution of *NBD*-P(OEGMA-*co*-DEGMA)-RhB_2 at 45 °C, under which condition thermoresponsive polymer chains are in the collapsed state and the FRET pair are quite close to each other. As the solution pH decreased from 10 to 2, we can apparently observe the appearance of a new emission band at

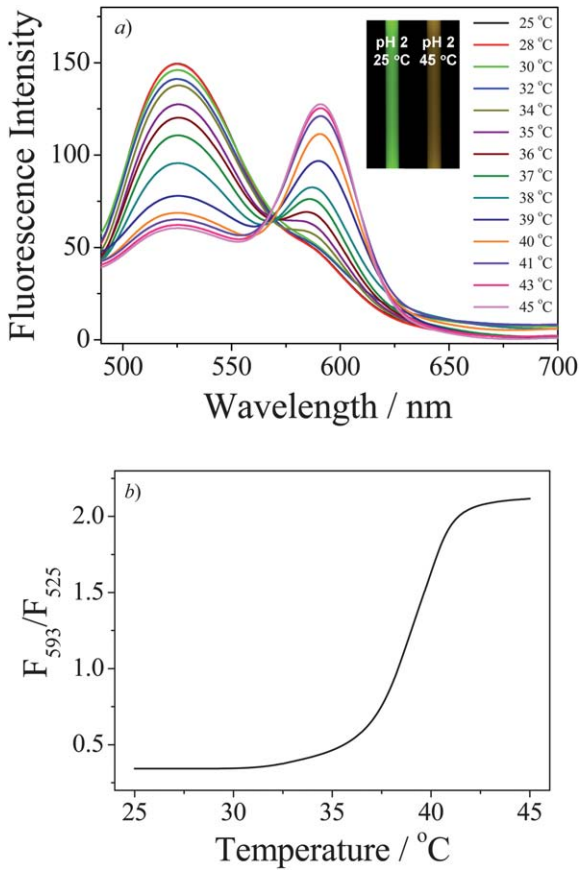

Fig. 6 (a) Fluorescence emission spectra and (b) fluorescence intensity ratio changes, F_{593}/F_{525}, recorded for 1.0 mg L^{-1} aqueous solution of *NBD*-P(OEGMA$_{0.06}$-*co*-DEGMA$_{0.94}$)$_{190}$- *RhB*$_2$ (pH 2, $\lambda_{ex} = 470$ nm; slit widths: Ex 5 nm, Em 5 nm) in the temperature range of 25–45 °C. The inset in (a) shows photographs recorded under inverted fluorescence microscopy equipped with a temperature-regulated incubator (450–480 nm exciter filter and long pass 515 nm barrier filter) for the aqueous solution of *NBD*-P(OEGMA$_{0.06}$-*co*-DEGMA$_{0.94}$)$_{190}$-*RhB*$_2$ at 25 °C and 45 °C (pH 2), respectively.

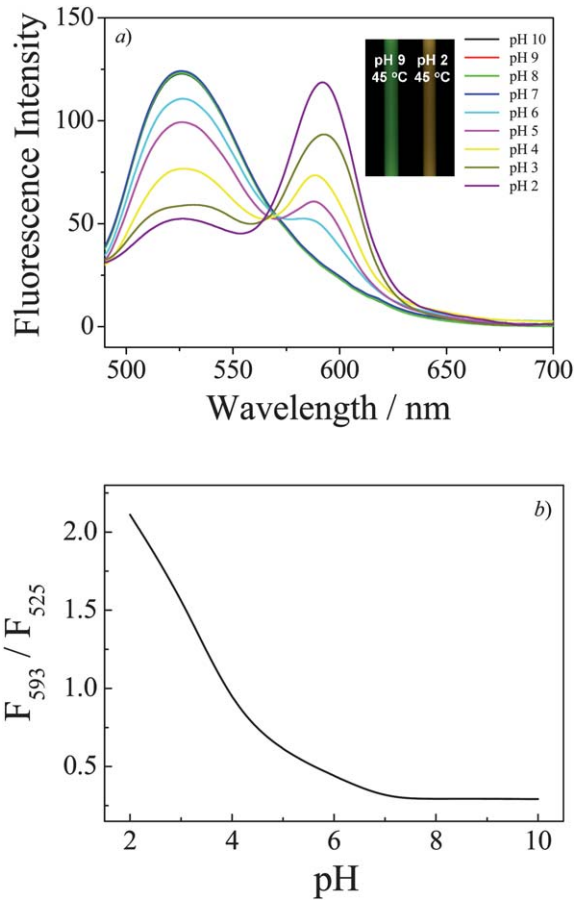

Fig. 7 (a) Fluorescence emission spectra and (b) fluorescence intensity ratio changes, F_{593}/F_{525}, recorded for 1.0 mg L^{-1} aqueous solution of *NBD*-P(OEGMA$_{0.06}$-*co*-DEGMA$_{0.94}$)$_{190}$- *RhB*$_2$ (45 °C, $\lambda_{ex} = 470$ nm; slit widths: Ex 5 nm, Em 5 nm) in the pH range of 2–10. The inset in (a) shows photographs recorded under inverted fluorescence microscopy equipped with a temperature-regulated incubator (450–480 nm exciter filter and long pass 515 nm barrier filter) for the aqueous solution of *NBD*-P(OEGMA$_{0.06}$-*co*-DEGMA$_{0.94}$)$_{190}$-*RhB*$_2$ at pH 2 and pH 9 (45 °C), respectively.

593 nm, and the intensity of which increases with decreasing pH values. This can be ascribed to the transformation of RhB residues from the non-fluorescent spirolactam form to the highly fluorescent acyclic form. On the other hand, the intensity decrease of NBD emission band at 525 nm with decreasing solution pH can be well-correlated to the occurrence of effective FRET processes between NBD and RhB moieties ($E \sim 62.6\%$, $F_{593}/F_{525} \sim 2.1$ at 45 °C). From Fig. 7, we can tell that the emission intensity ratio, F_{593}/F_{525}, at 45 °C increased from 0.29 at pH 10 to 2.1 at pH 2. Similarly, under an inverted fluorescence microscope, we can again observe the fluorometric green-to-orange transition as the solution pH decreased from 9 to 2. In the current system, thermo-induced collapse of single thermoresponsive polymer chains site-specifically labeled (chain middle and terminals) with FRET pair was employed to construct ratiometric fluorescent probes for pH and temperatures under highly dilute conditions by integrating the FRET principle with off/on pH-switchable emission characteristics of RhB-ethylenediamine moieties. Considering its structural integrity and effective and multifunctional sensing capabilities at such a low concentration, the current system is quite promising in the context of their applications in bio-sensing, imaging, and biomedicine fields.

4. Conclusions

We reported on the synthesis of dual ratiometric fluorescent probes for pH and temperatures based on single thermoresponsive polymer chains, *NBD*-P(OEGMA-*co*-DEGMA)-*RhB*$_2$, which were site-specifically labeled with FRET donor (NBD) and RhB-ethylenediamine derivative possessing off–on pH-switchable emission characteristics at the chain middle and terminals. The fluorescence emission of terminal RhB functionalities is highly pH-dependent, *i.e*, non-fluorescent in neutral or alkaline media (spirolactam form) and highly fluorescent in acidic media (ring-opened acyclic form), thus the off/on switching of FRET process can be facilely modulated by solution pH. Moreover, by taking advantage of the characteristic thermoresponsive properties *NBD*-P(OEGMA-*co*-DEGMA)-*RhB*$_2$ random copolymer

and its thermo-induced single chain collapsing behavior under highly dilute conditions, the variation in solution pH and temperatures can be accurately monitored by changes in fluorescence intensity ratios. The incorporation of one FRET donor and two pH-switchable acceptors at the chain middle and terminals of thermoresponsive polymers allows the effective off/on switching and the modulation of FRET efficiencies by dually playing with solution pH and temperatures. The reported dual ratiometric fluorescent probes for pH and temperature based on site-specifically FRET pair-labeled stimuli-responsive polymers display accurate and sensitive multiple detection capabilities under extremely dilute conditions, which augur well for their potential applications in biosensing and bioimaging.

Acknowledgements

The financial support from National Natural Scientific Foundation of China (NNSFC) Project (20874092, 91027026, and 51033005), Fundamental Research Funds for the Central Universities, and Specialized Research Fund for the Doctoral Program of Higher Education (SRFDP) is gratefully acknowledged.

References

1 B. B. Lowell and B. M. Spiegelman, *Nature*, 2000, **404**, 652–660.
2 L. E. Gerweck and K. Seetharaman, *Cancer Res.*, 1996, **56**, 1194–1198.
3 A. S. E. Ojugo, P. M. J. McSheehy, D. J. O. McIntyre, C. McCoy, M. Stubbs, M. O. Leach, I. R. Judson and J. R. Griffiths, *NMR Biomed.*, 1999, **12**, 495–504.
4 J. Y. Han and K. Burgess, *Chem. Rev.*, 2010, **110**, 2709–2728.
5 D. M. Monti, L. Brandt, J. Ikomi-Kumm and H. Olsson, *Scand. J. Haematol.*, 1986, **36**, 353–357.
6 M. Karnebogen, D. Singer, M. Kallerhoff and R. H. Ringert, *Thermochim. Acta*, 1993, **229**, 147–155.
7 Y. Urano, D. Asanuma, Y. Hama, Y. Koyama, T. Barrett, M. Kamiya, T. Nagano, T. Watanabe, A. Hasegawa, P. L. Choyke and H. Kobayashi, *Nat. Med.*, 2009, **15**, 104–109.
8 B. Tang, F. Yu, P. Li, L. L. Tong, X. Duan, T. Xie and X. Wang, *J. Am. Chem. Soc.*, 2009, **131**, 3016–3023.
9 X. J. Wan, D. Wang and S. Y. Liu, *Langmuir*, 2010, **26**, 15574–15579.
10 J. Y. Zhang, Y. T. Li, S. P. Armes and S. Y. Liu, *J. Phys. Chem. B*, 2007, **111**, 12111–12118.
11 F. Galindo, M. I. Burguete, L. Vigara, S. V. Luis, N. Kabir, J. Gavrilovic and D. A. Russell, *Angew. Chem., Int. Ed.*, 2005, **44**, 6504–6508.
12 E. Pringsheim, D. Zimin and O. S. Wolfbeis, *Adv. Mater.*, 2001, **13**, 819–822.
13 Q. Yan, J. Y. Yuan, W. Z. Yuan, M. Zhou, Y. W. Yin and C. Y. Pan, *Chem. Commun.*, 2008, 6188–6190.
14 S. Charier, O. Ruel, J. B. Baudin, D. Alcor, J. F. Allemand, A. Meglio and L. Jullien, *Angew. Chem., Int. Ed.*, 2004, **43**, 4785–4788.
15 H. S. Peng, J. A. Stolwijk, L. N. Sun, J. Wegener and O. S. Wolfbeis, *Angew. Chem., Int. Ed.*, 2010, **49**, 4246–4249.
16 C. Pietsch, R. Hoogenboom and U. S. Schubert, *Angew. Chem., Int. Ed.*, 2009, **48**, 5653–5656.
17 L. Albertazzi, B. Storti, L. Marchetti and F. Beltram, *J. Am. Chem. Soc.*, 2010, **132**, 18158–18167.
18 J. Yin, H. B. Hu, Y. H. Wu and S. Y. Liu, *Polym. Chem.*, 2011, **2**, 363–371.
19 J. Yin, C. H. Li, D. Wang and S. Y. Liu, *J. Phys. Chem. B*, 2010, **114**, 12213–12220.
20 H. Sun, A. M. Scharff-Poulsen, H. Gu and K. Almdal, *Chem. Mater.*, 2006, **18**, 3381–3384.
21 S. Hornig, C. Biskup, A. Grafe, J. Wotschadlo, T. Liebert, G. J. Mohr and T. Heinze, *Soft Matter*, 2008, **4**, 1169–1172.
22 S. Modi, M. G. Swetha, D. Goswami, G. D. Gupta, S. Mayor and Y. Krishnan, *Nat. Nanotechnol.*, 2009, **4**, 325–330.
23 C. D. H. Alarcon, S. Pennadam and C. Alexander, *Chem. Soc. Rev.*, 2005, **34**, 276–285.
24 C. Gota, K. Okabe, T. Funatsu, Y. Harada and S. Uchiyama, *J. Am. Chem. Soc.*, 2009, **131**, 2766–2767.
25 Y. Shiraishi, R. Miyarnoto and T. Hirai, *Langmuir*, 2008, **24**, 4273–4279.
26 S. Uchiyama, N. Kawai, A. P. de Silva and K. Iwai, *J. Am. Chem. Soc.*, 2004, **126**, 3032–3033.
27 A. Nagai, K. Kokado, J. Miyake and Y. Cyujo, *J. Polym. Sci., Part A: Polym. Chem.*, 2010, **48**, 627–634.
28 T. Liu, J. M. Hu, J. Yin, Y. F. Zhang, C. H. Li and S. Y. Liu, *Chem. Mater.*, 2009, **21**, 3439–3446.
29 J. Yin, X. F. Guan, D. Wang and S. Y. Liu, *Langmuir*, 2009, **25**, 11367–11374.
30 L. Tang, J. K. Jin, A. J. Qin, W. Z. Yuan, Y. Mao, J. Mei, J. Z. Sun and B. Z. Tang, *Chem. Commun.*, 2009, 4974–4976.
31 Z. Q. Guo, W. H. Zhu, Y. Y. Xiong and H. Tian, *Macromolecules*, 2009, **42**, 1448–1453.
32 Y. Shen, M. Kuang, Z. Shen, J. Nieberle, H. W. Duan and H. Frey, *Angew. Chem., Int. Ed.*, 2008, **47**, 2227–2230.
33 J. M. Hu, C. H. Li and S. Y. Liu, *Langmuir*, 2010, **26**, 724–729.
34 T. Wu, G. Zou, J. M. Hu and S. Y. Liu, *Chem. Mater.*, 2009, **21**, 3788–3798.
35 A. Nagai, R. Yoshii, T. Otsuka, K. Kokado and Y. Chujo, *Langmuir*, 2010, **26**, 15644–15649.
36 T. Förster, *Modern Quantum Chemistry*, O. Sinanoglu, Ed.; Academic Press: New York, 1965; part III, p1993.
37 G. D. Scholes, *Annu. Rev. Phys. Chem.*, 2003, **54**, 57–87.
38 M. Beija, M. T. Charreyre and J. M. G. Martinho, *Prog. Polym. Sci.*, 2011, **36**, 568–602.
39 J. M. Hu and S. Y. Liu, *Macromolecules*, 2010, **43**, 8315–8330.
40 H. N. Kim, Z. Q. Guo, W. H. Zhu, J. Yoon and H. Tian, *Chem. Soc. Rev.*, 2011, **40**, 79–93.
41 S. W. Hong, K. H. Kim, J. Huh, C. H. Ahn and W. H. Jo, *Chem. Mater.*, 2005, **17**, 6213–6215.
42 S. W. Hong, D. Y. Kim, J. U. Lee and W. H. Jo, *Macromolecules*, 2009, **42**, 2756–2761.
43 P. J. Roth, M. Haase, T. Basche, P. Theato and R. Zentel, *Macromolecules*, 2010, **43**, 895–902.
44 Y. Shiraishi, R. Miyamoto, X. Zhang and T. Hirai, *Org. Lett.*, 2007, **9**, 3921–3924.
45 Y. Xiang and A. J. Tong, *Org. Lett.*, 2006, **8**, 1549–1552.
46 C. H. Li, Y. X. Zhang, J. M. Hu, J. J. Cheng and S. Y. Liu, *Angew. Chem., Int. Ed.*, 2010, **49**, 5120–5124.
47 P. Wu, M. Malkoch, J. N. Hunt, R. Vestberg, E. Kaltgrad, M. G. Finn, V. V. Fokin, K. B. Sharpless and C. J. Hawker, *Chem. Commun.*, 2005, 5775–5777.
48 J. H. Soh, K. M. K. Swamy, S. K. Kim, S. Kim, S. H. Lee and J. Yoon, *Tetrahedron Lett.*, 2007, **48**, 5966–5969.
49 M. Onoda, S. Uchiyama, T. Santa and K. Imai, *Anal. Chem.*, 2002, **74**, 4089–4096.
50 J. F. Lutz, O. Akdemir and A. Hoth, *J. Am. Chem. Soc.*, 2006, **128**, 13046–13047.
51 J. F. Lutz and A. Hoth, *Macromolecules*, 2006, **39**, 893–896.
52 S. Han, M. Hagiwara and T. Ishizone, *Macromolecules*, 2003, **36**, 8312–8319.
53 H. G. Schild, *Prog. Polym. Sci.*, 1992, **17**, 163–249.
54 G. B. Sun and Z. B. Guan, *Macromolecules*, 2010, **43**, 9668–9673.
55 S. W. Hong and W. H. Jo, *Polymer*, 2008, **49**, 4180–4187.
56 E. S. Cho, S. W. Hong and W. H. Jo, *Macromol. Rapid Commun.*, 2008, **29**, 1798–1803.
57 S. W. Hong, C. H. Ahn, J. Huh and W. H. Jo, *Macromolecules*, 2006, **39**, 7694–7700.
58 J. U. Lee, A. Cirpan, T. Emrick, T. P. Russell and W. H. Jo, *J. Mater. Chem.*, 2009, **19**, 1483–1489.
59 S. Uchiyama, Y. Matsumura, A. P. de Silva and K. Iwai, *Anal. Chem.*, 2003, **75**, 5926–5935.
60 S. Uchiyama, Y. Matsumura, A. P. de Silva and K. Iwai, *Anal. Chem.*, 2004, **76**, 1793–1798.
61 C. Gota, S. Uchiyama, T. Yoshihara, S. Tobita and T. Ohwada, *J. Phys. Chem. B*, 2008, **112**, 2829–2836.
62 S. Y. Lee, S. Lee, I. C. Youn, D. K. Yi, Y. T. Lim, B. H. Chung, J. F. Leary, I. C. Kwon, K. Kim and K. Choi, *Chem.–Eur. J.*, 2009, **15**, 6103–6106.